Gaussian Process Based Method for Point and Probabilistic Short-Term Wind Power Forecast

Ali Lahouar(✉)

Laboratory of Advanced Technology and Intelligent Systems (LATIS), National Engineering School of Sousse (ENISO), University of Sousse, Sousse, Tunisia
ali.lahouar@eniso.rnu.tn

Abstract. Wind power is becoming one of the most promising renewable energy sources. With a total capacity exceeding 486 gigawatts worldwide in 2016, wind power optimization, forecast and control become more challenging than ever before. Forecasting wind turbines output for a period of time in advance is beneficial for grid managers, since it allows them to optimize their generation plans and to control the production of conventional thermal or nuclear plants. This paper proposes then a Gaussian process based method for predicting the production of a wind farm for one and two hours in advance. Both point and probabilistic forecasts are performed through customizable prediction intervals with different confidence levels. The model is tested using real data from Sidi Daoud wind farm in northeast Tunisia. Results are analyzed and compared to similar methods in terms of various assessment metrics.

Keywords: Wind power forecast · Short term · Wind speed and direction · Gaussian process · Probabilistic forecast · Prediction intervals

1 Introduction

Efficient exploitation of energy resources becomes more challenging in modern grids, with the increasing penetration levels of renewable generation worldwide. Optimized control of wind farms in particular is difficult due to wind intermittence and complexity of weather patterns. Accurate forecast of future wind power is therefore mandatory to ensure continuous and stable electricity supply. Indeed, intermittent generation can inject disturbances into the grid, and may cause frequency regulation problems. Probabilistic forecast is able to generate different possible outcomes of future power, in order to take into account several possible scenarios. The transition from deterministic to probabilistic predictions is mandatory because of uncertainties associated with electricity generation and trade. In fact, probabilistic forecast is a powerful tool to manage power reserves and to optimize bidding strategies.

M. S. Bouhlel and S. Rovetta (Eds.): SETIT 2018, SIST 147, pp. 134–147, 2020.
https://doi.org/10.1007/978-3-030-21009-0_12

New schemes for security evaluation are proposed in the literature to take into account the disturbances induced by intermittent generation [1]. Among these disturbances, previous research papers cite the effects on voltage stability [2]. The impact of wind forecast uncertainty on power systems is likewise evaluated [3]. Under these circumstances, probabilistic forecast shows a high flexibility. Indeed, it is proven that probabilistic wind power prediction can contribute to efficient operation of electricity markets with high penetration levels [4]. Probabilistic wind power forecast facilitates several tasks in modern power grids, such as optimal setting of operating reserves [5], predictive control of battery energy storage system [6], and unit commitment [7].

The state of the art of probabilistic wind power forecasting is already well developed. A review of different methods can be found easily in the literature [8]. Most methods make use of either physical or statistical models. Physical models are generally based on numerical weather prediction, while statistical methods focus mainly on time series. Artificial intelligence, machine learning, and heuristic optimization are common approaches to deal with wind power and speed forecast. For example, a framework based on the particle filter algorithm is applied to predict the output of each wind farm apart [9]. Fuzzy k-means clustering algorithm, support vector regression and quantile regression are utilized in a probabilistic forecast framework [10]. Quantile regression is also combined with extreme learning machine to generate nonparametric probabilistic forecasting, where quantiles are produced using a linear programming optimization model [11]. A method based on Gaussian process, making use of a local moving window, is also proposed for this purpose [12]. Variants of this method are also proposed, such as warped Gaussian process [13]. The k-nearest neighbors algorithm is likewise utilized in probabilistic forecasting, either alone [14] or combined with kernel density estimator [15]. Quantile regression for probabilistic prediction is performed using a reproducing kernel Hilbert space framework [16]. Double seasonal Holt Winters and conditional density kernel estimation are developed in order to estimate the probabilistic density of wind power [17]. Sparse Bayesian learning and discrete wavelet transform are carried out in order to solve the problem of wind power forecast [18]. Several other methods are also developed, such as gradient boosting machine [19], radial basis function neural networks [20], kernel density estimator with logarithmic transformation [21], Markov chain models [22], and sparse vector autoregression [23]. The abundance of sophisticated methods proves the importance of probabilistic power prediction and justifies the need for more advanced approaches to handle the increasing uncertainty.

This paper proposes a short-term probabilistic wind power forecast based on Gaussian process (GP). The method itself has already been used before. The novelty, however, lies in the selection of inputs, commonly called features. In order to take into consideration the spatial correlation between wind turbines, the wind speed is averaged spatially and used as input. The wind direction is also appended to the input vector. It will be proved that wind direction and spatially averaged speed affect the overall farm production. The lead time is set to 1 and

2 h in advance. Nine prediction intervals are provided by the GP model according to confidence levels ranging from 10% to 90%. Various evaluation metrics are suggested to assess the forecast accuracy. To our best knowledge, the effects of spatially averaged wind speed and direction in a Gaussian process forecaster were not assessed before this work. The remainder of the paper is organized as follows. Section 2 defines the forecast methodology, Sect. 3 presents and discusses results, and Sect. 4 concludes the paper.

2 Forecast Methodology

2.1 Data Preprocessing

Renewable energy and smart grid technologies in Tunisia are getting more and more attention by researchers [24,25], since they are in continuous development. Therefore, the data used in this work will be taken from Sidi Daoud wind farm in northeast Tunisia. The total installed capacity is 53.5 MW. The rated power of the 70 wind turbines in the farm ranges from 330 kW to 1320 kW. Turbines are aligned from northeast to southwest, perpendicularly to the wind dominant direction. The wind speed is metered above the nacelle of each individual wind turbine apart. The wind direction is measured from the meteorological mast inside the farm, in addition to temperature, relative humidity and atmospheric pressure. The power output of each turbine, in addition to the aforementioned meteorological factors, are given in the form of time series sampled at 10 min for the years 2010 and 2011.

The huge amount of data includes necessarily some errors. The preprocessing is therefore mandatory. Major corrections are: filling gaps (missing samples) with previous values, removing redundant and repeated samples, and avoiding sensors failure periods (large periods with immovable or inconsistent values). In addition, the overall produced power output of the farm is calculated, by summing the power outputs of all turbines. Time series averaging is also proposed in order to get new quantities. The averaging is either spatial, or temporal. Spatial averaging is obtained by calculating the mean of 70 wind speed measures, in order to benefit from spatial smoothing effect. It is proven in Fig. 1 that the spatially averaged speed is more correlated to the farm power output than the speed metered by the meteorological tower. Temporal averaging is applied to the power output, where each consecutive six values are replaced by their mean. This operation provides smoother curves, and thus easier to predict.

2.2 Feature Selection

The feature selection is the process of choosing the appropriate inputs of the forecaster. Let X be the input vector, and $\hat{Y}$ the provided output distribution, intended to estimate the real output Y. In this paper, the lead time, or forecast horizon, is set to 1 and 2 h in advance. Therefore, all features will be selected from hour h in order to predict power at hour $h+1$ or $h+2$. Let S be the wind

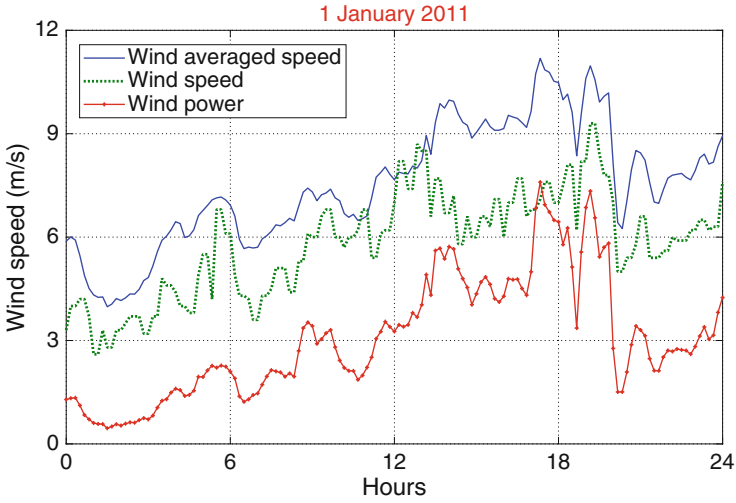

Fig. 1. Wind spatially averaged speed (solid curve), wind speed from the weather mast (dotted curve), and overall power output (solid curve with dots) on January 1st, 2011

speed, D the wind direction, and P the wind power. $\bar{S}$ will be used to denote the spatially averaged wind speed (mean of 70 measures), and $\tilde{P}$ to denote the temporal average of power output (mean of six consecutive values). Six values of each quantity in $\{P, \bar{S}, D\}$ at hour h (from $h:00$ to $h:50$), will be selected to predict the average power $\tilde{P}$ at hour $h+1$ or $h+2$. The input vector X, is then expressed as follows:

$$X = [P_{h:00}, \ldots, P_{h:50}, \bar{S}_{h:00}, \ldots \bar{S}_{h:50}, D_{h:00}, \ldots, D_{h:50}]^T \tag{1}$$

Where $P_{h:00}$ is the power measured at $h:00$, $D_{h:30}$ is the wind direction metered at $h:30$, and so on. The total number of inputs is therefore 18. The average power $\tilde{P}_h$ at hour h is naturally given by:

$$\tilde{P}_h = \frac{1}{6} \sum_{i=0}^{5} P_{h:i0} \tag{2}$$

The output $\hat{Y}$ provided by the GP forecaster, should be an estimation $\hat{\tilde{P}}$ of $\tilde{P}$ at hour $h+1$ or $h+2$, according to the required forecast horizon.

$$\hat{Y} = \hat{\tilde{P}}_{h+1} \quad \text{or} \quad \hat{Y} = \hat{\tilde{P}}_{h+2} \tag{3}$$

Past values of power are utilized according to the autocorrelation plot of Fig. 2, which is extended to include 24 past hours. The autocorrelation reveals the similarities between the power time series and its lagged version. Lags with maximum similarity are those close to zero. Even with a lag of three hours, the correlation is still higher than 0.8. Therefore, it is judicious to utilize the six

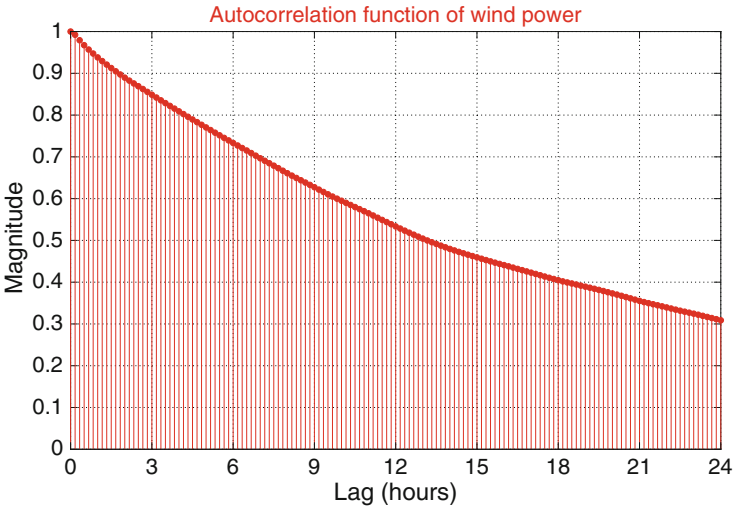

Fig. 2. Autocorrelation plot of wind power time series, sampled at 10 min

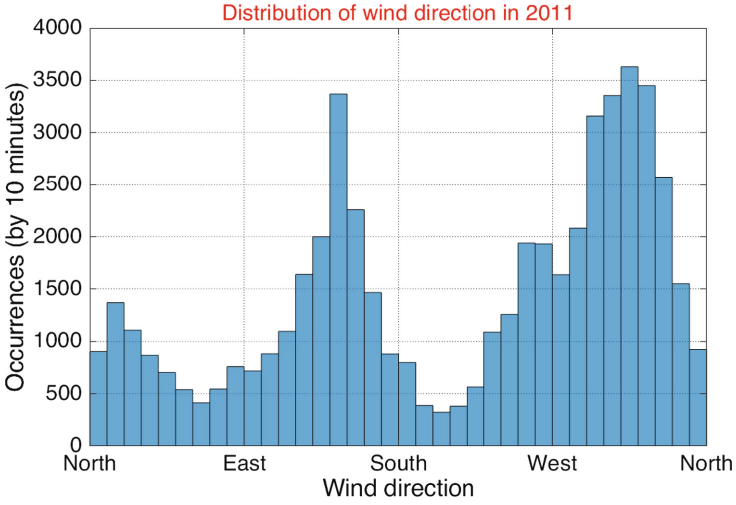

Fig. 3. Histogram of wind direction samples in 2011

power measurements at the current hour h in order to predict the average power of the next hours $h+1$ and $h+2$.

The spatially averaged wind speed $\bar{S}$ is the second category of inputs. It is selected according to Fig. 1, where its correlation with power output is obvious. Consequently, it has certainly a great impact on the generated power. The third family of inputs, which is the wind direction D, affects also the power output. The distribution of wind direction occurrences in 2011 are given in Fig. 3, recorded

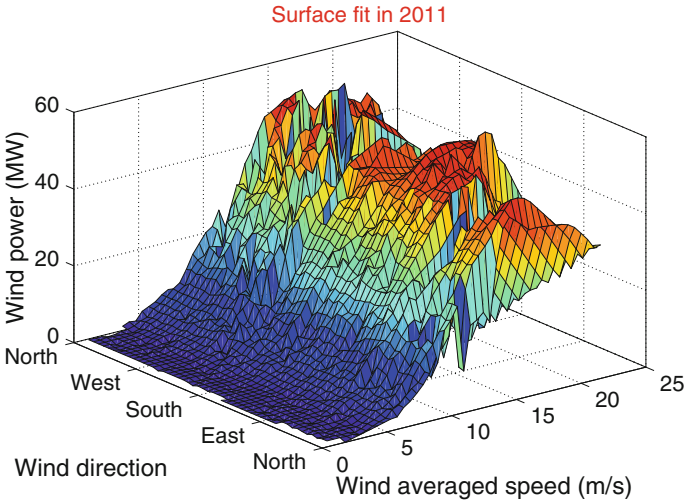

Fig. 4. Surface plot of wind power fitted to averaged speed and direction in 2011

each 10 min throughout the year. Major directions are northwest and southeast, which are perpendicular to the turbines alignment in the farm. It is therefore expected that power is maximum for these directions in particular, and minimum elsewhere. The surface plot of Fig. 4 asserts this assumption, where the generated power is fitted to wind speed and direction. Obviously, the average wind speed is the most influential factor that drives the power output. However, at the rated speed of 15 m/s, some peaks and valleys appear on the surface according to wind direction. Indeed, peaks of power arise for northwest and southeast directions, while power valleys dominate the remainder.

2.3 Mapping Function

This section describes the input/output mapping function of the Gaussian process (GP). The GP has several advantages. It is probabilistic; different prediction intervals can be constructed according to different confidence levels. Furthermore, it is versatile. Different kernels may be specified according to a covariance function. The GP is utilized in this paper for supervised regression. Let S_n be a training set containing n observations $S_n = \{(X_1, Y_1), \ldots, (X_i, Y_i), ..., (X_n, Y_n)\}$, where X_i is a vector of dimension d ($d = 18$ in this paper), and Y_i is the corresponding scalar target. The set may be written $S_n = \{X, Y\}$, where X is a $d \times n$ matrix. Let X^* be an unseen input vector, i.e. does not belong to S_n. The aim of the prediction is to determine the output scalar Y^* that corresponds to this new input. According to the GP, the target Y^* follows a normal distribution [26]:

$$Y^* \sim \mathcal{N}(\mu, \sigma^2) \tag{4}$$

Where:

$$\mu = K(X, X^*)K(X, X)^{-1}Y \tag{5}$$

$$\sigma = K(X^*, X^*) - K(X, X^*)K(X, X)^{-1}K(X^*, X) \tag{6}$$

K is a covariance function, for example the squared exponential:

$$K(X, X^*) = \exp\left(-\frac{1}{2}|X - X^*|^2\right) \tag{7}$$

$\mathcal{N}$ is the normal distribution, whose probability density f is given by:

$$f(x) = \frac{1}{\sqrt{2\pi\sigma^2}} \exp\left(-\frac{(x-\mu)^2}{2\sigma^2}\right) \tag{8}$$

Several prediction intervals may be obtained from Y^* through quantiles. Let F be the cumulative distribution function of the random variable Y^*. The α^{th} quantile of Y^* is given by [27]:

$$Q_{Y^*}(\alpha) = F_{Y^*}^{-1}(\alpha) = inf\{y : F_{Y^*}(y) \geq \alpha\}; y \in \mathbb{R} \tag{9}$$

Where $0 \leq \alpha \leq 1$. For example, the $Q_{Y^*}(0.6)$ is the quantile below which 60% of Y^* observations are expected. Prediction intervals (PI) are constructed from quantiles according to confidence levels. For instance, the PI associated to the confidence level 80% is defined by:

$$PI_{80\%}(Y^*) = [Q_{Y^*}(0.10), Q_{Y^*}(0.90)] \tag{10}$$

The median value $Q_{Y^*}(0.50)$ will be utilized for point forecast and for comparison with similar methods. Nine PI are constructed for probabilistic forecast, ranging from 10% to 90%.

3 Case Study

3.1 Assessment Metrics

In order to evaluate quantitatively the prediction accuracy, several metrics are already in use by researchers. For point forecast provided by the median value $Q_{Y^*}(0.50)$, four assessment criteria are proposed in this paper. They are the mean absolute error (MAE), the root mean squared error ($RMSE$), the mean absolute percentage error ($MAPE$) and the mean absolute scaled error ($MASE$), defined by:

$$MAE = \frac{1}{s}\sum_{i=1}^{s}|\hat{P}_i - P_i| \tag{11}$$

$$RMSE = \sqrt{\frac{1}{s}\sum_{i=1}^{s}(\hat{P}_i - P_i)^2} \tag{12}$$

$$MAPE = \frac{1}{s}\sum_{i=1}^{s}\frac{|\hat{P}_i - P_i|}{P_s} \times 100 \tag{13}$$

$$MASE = \frac{1}{s}\sum_{i=1}^{s}\left(\frac{|\hat{P}_i - P_i|}{\frac{1}{s-1}\sum_{j=2}^{s}|P_j - P_{j-1}|}\right) \tag{14}$$

Where s is the number of hours in the testing period. For each hour h, the quantity $\hat{P}_i$ stands for the predicted average power $\hat{\tilde{P}}_{h+1}$ or $\hat{\tilde{P}}_{h+2}$ provided by the GP median value $Q_{Y^*}(0.50)$, according the prediction horizon. Naturally, P_i denotes the actual measured average power $\tilde{P}_{h+1}$ or $\tilde{P}_{h+2}$, also according to the forecast horizon. P_s is the actual power averaged over the whole test period, $P_s = \frac{1}{s}\sum_{i=1}^{s} P_i$. Two additional metrics are suggested for probabilistic forecast, which are the Pinball loss function (PLF), and the Winkler score (WS). The PLF is defined for each quantile $Q_{Y^*}(\alpha)$ by [28]:

$$PLF(Q_{Y^*}(\alpha)) = \tag{15}$$
$$\begin{cases} (1-\alpha)(Q_{Y^*}(\alpha) - P_i) & if\ P_i < Q_{Y^*}(\alpha) \\ \alpha(P_i - Q_{Y^*}(\alpha)) & if\ P_i \geq Q_{Y^*}(\alpha) \end{cases}$$

Where $\alpha \in \{0.1, 0.2, ..., 0.9\}$. In addition, let $PI_{c\%}(Y^*)$ be the prediction interval associated to the confidence level $c\% = (1-2\alpha) \times 100$:

$$PI_{c\%}(Y^*) = [Q_{Y^*}(\alpha), Q_{Y^*}(1-\alpha)] \tag{16}$$

Where $\alpha \in \{0.05, 0.10, ..., 0.45\}$. The width of $PI_{c\%}(Y^*)$ is denoted $\delta_{c\%}$, with $\delta_{c\%} = Q_{Y^*}(1-\alpha) - Q_{Y^*}(\alpha)$. The WS is defined by [28]:

$$WS(PI_{c\%}(Y^*)) = \tag{17}$$
$$\begin{cases} \delta_{c\%} & for\ P_i \in PI_{c\%}(Y^*) \\ \delta_{c\%} + \frac{1}{\alpha}(Q_{Y^*}(\alpha) - P_i) & for\ P_i < Q_{Y^*}(\alpha) \\ \delta_{c\%} + \frac{1}{\alpha}(P_i - Q_{Y^*}(1-\alpha)) & for\ P_i > Q_{Y^*}(1-\alpha) \end{cases}$$

All proposed metrics are proposed to quantify the distance between real and predicted samples, but from different points of view.

3.2 Results and Discussion

The aforementioned GP forecaster is tested for a lead time of 1 h in advance, on four different weeks in 2011. The seven first days, 1st to 7th day of February, May, August and November, are selected for this purpose. Test periods are selected intentionally across different seasons in order to verify the prediction accuracy under different circumstances. Forecast results are given in Fig. 5 in the form of fan plot, for August and November only. Only four days of each period are shown for sake of clarity. Actual power is represented by the dashed curve, whereas point forecast is represented by the solid curve. The nine prediction intervals, ranging

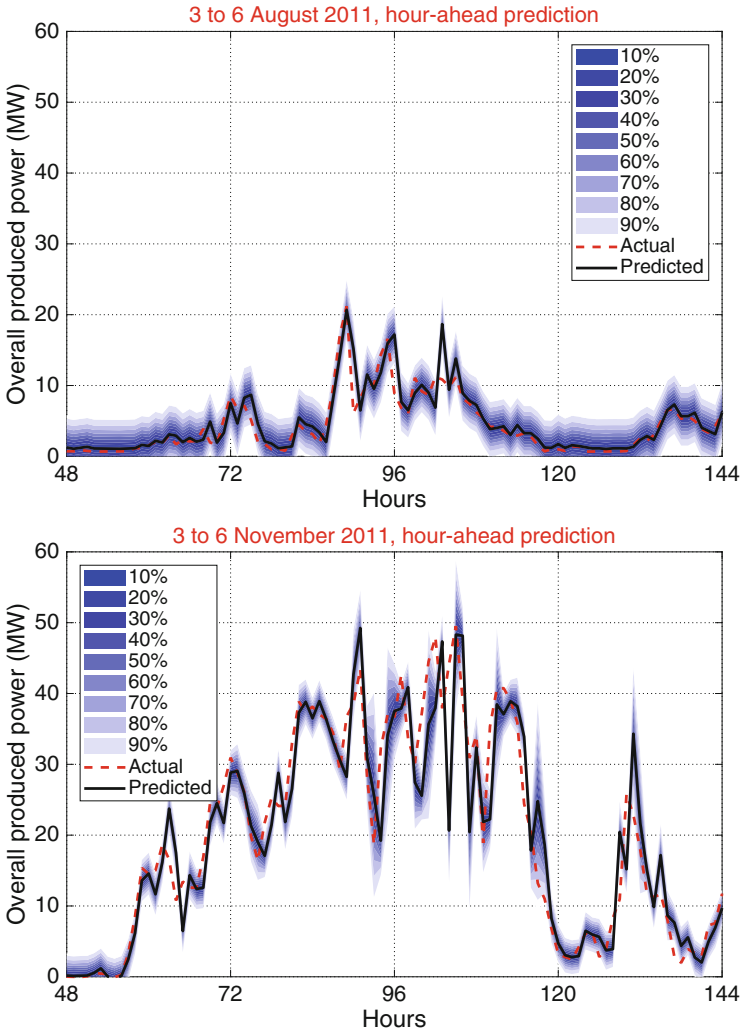

Fig. 5. Actual curve and prediction intervals of one hour ahead wind power forecast

from 10% to 90%, are given in the form of color gradient. The darkest color stands for the narrower PI (10%), and the lighter color stands for the wider PI (90%).

For this short lead time of 1 h in advance, results of point forecast are already satisfactory. With the exception of some sudden and very sharp variations, the predicted curve succeeds to follow the major trends of the actual curve. Forecast accuracy is verified under different scenarios, even with very spiky curves like those of November, or abnormally low production like that of August. The GP is compared to some conventional prediction methods, namely persistence (PER),

artificial neural networks (ANN) and support vector machines (SVM). Comparison is performed in terms of the four aforementioned metrics, *MAE*, *RMSE*, *MAPE*, and *MASE*. Results are given in Table 1, where all metrics are computed on the first 7 days of each test month. With the exception of November, the GP gives always the lower error. In fact, the special spiky curve in November makes the prediction more difficult.

Table 1. Evaluation metrics of one hour ahead point forecast using four different methods

Period	1 to 7 February				1 to 7 May			
Criterion	PER	ANN	SVM	GP	PER	ANN	SVM	GP
MAE	2.9533	2.7317	4.2068	2.3509	3.8553	2.9549	3.9594	2.8284
RMSE	4.2109	4.3042	7.0569	3.6503	5.7793	4.3870	5.8416	4.3202
MAPE	14.1811	13.1170	20.2002	11.2883	17.0541	13.0710	17.5148	12.5114
MASE	1.0036	0.9283	1.4296	0.7989	0.9956	0.7631	1.0225	0.7304
Period	1 to 7 August				1 to 7 November			
Criterion	PER	ANN	SVM	GP	PER	ANN	SVM	GP
MAE	1.2273	1.1110	1.7525	0.9724	3.0585	2.6699	4.2139	3.0737
RMSE	2.0932	1.6665	2.6286	1.5260	4.5172	4.2176	7.6371	4.8488
MAPE	25.6834	23.2499	36.6736	20.3498	19.7480	17.2389	27.2086	19.8463
MASE	1.0116	0.9158	1.4445	0.8015	1.0024	0.8750	1.3811	1.0074

Table 2. Evaluation metrics of one hour ahead probabilistic forecast

PLF	February	May	August	November	*WS*	February	May	August	November
0.10	0.6411	0.7327	0.4172	0.7069	90%	11.1283	10.8624	9.3174	8.6480
0.20	0.9153	1.0901	0.5379	1.0374	80%	8.6704	8.4632	7.2595	6.7379
0.30	1.0766	1.2905	0.5334	1.2514	70%	7.0120	6.8445	5.8710	5.4492
0.40	1.1879	1.3849	0.4675	1.3902	60%	5.6940	5.5580	4.7674	4.4249
0.50	1.2417	1.4050	0.4837	1.4681	50%	4.5633	4.4543	3.8207	3.5462
0.60	1.2650	1.3898	0.5780	1.4841	40%	3.5478	3.4631	2.9705	2.7414
0.70	1.2307	1.3045	0.6063	1.4136	30%	2.6069	2.5446	2.1827	1.7314
0.80	1.0798	1.1272	0.5596	1.2384	20%	1.7140	1.6731	1.4351	1.1207
0.90	0.7788	0.8144	0.4012	0.9287	10%	0.8502	0.8299	0.7118	0.6237

The probabilistic forecast is useful in the presence of some shifts between actual and predicted curves. In many cases, this shift is compensated by prediction intervals. This compensation, albeit not very clear, can be observed in

February and May in Fig. 5. Indeed, prediction intervals for a lead time of one hour in advance are narrow, and therefore their usefulness does not show up properly. The *PLF* and *WS* are computed in order to evaluate the prediction accuracy. Results appear in Table 2. The *PLF* is evaluated for each quantile, where $\alpha \in \{0.1, 0.2, ..., 0.9\}$, and averaged over the whole test period of 7 days in each month. In a similar manner, the *WS* is calculated for each prediction interval, with confidence levels ranging from 10% to 90%. It is likewise averaged over the whole test period. For both criteria, lower values reflect more accurate prediction. The *PLF*, for all quantiles, has lower values in August. Since the *PLF* characterizes only the forecast sharpness, it is expected that August results will be the best. Indeed, the actual power curve in August is much less spiky than other months, and it is consequently more predictable. However, the *WS* is minimum in November. In fact, the *WS* depends on PI widths. Since November PI are very narrow, the November *WS* is naturally lower than that of other months.

Table 3. Evaluation metrics of two hours ahead probabilistic forecast

PLF	February	May	*WS*	February	May
0.10	1.0860	1.4228	90%	19.8559	19.3694
0.20	1.6272	2.0687	80%	15.4703	15.0913
0.30	1.9315	2.4245	70%	12.5113	12.2048
0.40	2.1278	2.5777	60%	10.1597	9.9107
0.50	2.2303	2.6351	50%	8.1421	7.9426
0.60	2.2167	2.6351	40%	6.3303	6.1752
0.70	2.1191	2.4954	30%	4.6514	4.5374
0.80	1.8663	2.1713	20%	3.0583	2.9834
0.90	1.3594	1.5628	10%	1.5169	1.4798

Figure 6 shows the forecast results for a lead time of two hours in advance, from the 1st to the 7th day of February and May 2011. In this case, the point prediction encounters some difficulties. In many cases, a shift of one or two hours appear between actual and predicted curves. In this case, prediction intervals reveal their advantages. With larger bounds than those of hour-ahead forecast, PI are able to cover the actual curve in most cases. In February for example, the dashed curve is almost always covered by at least one PI, with the exception of the spectacular increase at the first hours of 3th February. The same phenomenon is observed in May. The inconvenient that may be cited here, is that very spiky curves cannot be followed easily even in the presence of different PI. However, the forecast accuracy is pretty satisfactory, and it is far away from point prediction in terms of sharpness. The *PLF* and *WS* are computed in case of two hours ahead prediction for the seven first days of February and May. The results, for each quantile and PI, are given in Table 3. Values of *PLF* and *WS* are a bit

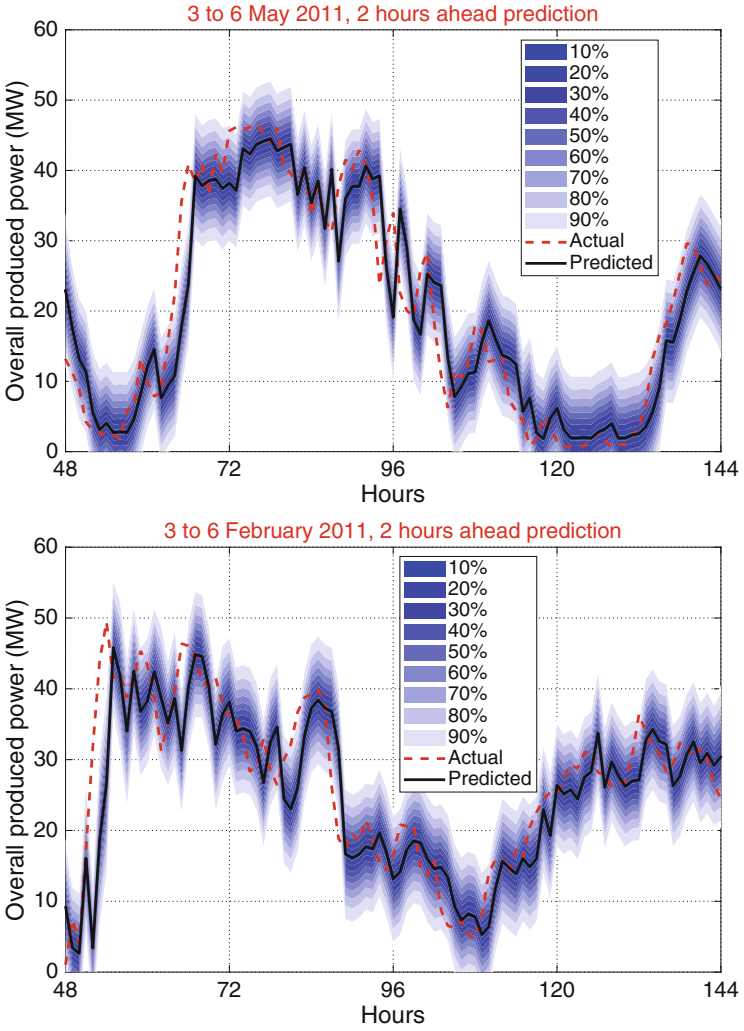

Fig. 6. Actual curve and prediction intervals of two hours ahead wind power forecast

higher now, which is expected for longer forecast horizons. In terms of *PLF*, the prediction in February, with respect to May, is somehow better. Nevertheless, in terms of *WS*, both months are almost equal.

4 Conclusion

This paper proposed a short-term wind power forecasting approach based on Gaussian process (GP). The GP is a probabilistic and versatile method, able to provide several prediction intervals with different confidence levels. The forecast

methodology was organized as follows. First, a set of wind power, speed and direction from a wind farm in Tunisia is considered and processed. Then, an analysis is carried out in order to select the best candidates to the forecaster input. Finally, an input/output mapping function is built using the GP specific equations. The output of the model was utilized for one hour and two hours of prediction in advance. In both cases, the GP forecaster shows very satisfying results in terms of several evaluation metrics. The future work involves the optimization of GP parameters, and the refinement of inputs with the intention of improving the forecast accuracy.

References

1. Le, D., Berizzi, A., Bovo, C.: A probabilistic security assessment approach to power systems with integrated wind resources. Renew. Energy **85**, 114–123 (2016)
2. Bian, X., Geng, Y., Yuan, F., Lo, K.L., Fu, Y.: Identification and improvement of probabilistic voltage instability modes of power system with wind power integration. Electric Power Syst. Res. **140**, 162–172 (2016)
3. Xydas, E., Qadrdan, M., Marmaras, C., Cipcigan, L., Jenkins, N., Ameli, H.: Probabilistic wind power forecasting and its application in the scheduling of gas-fired generators. Appl. Energy **192**, 382–394 (2017)
4. Botterud, A., Zhou, Z., Wang, J., Sumaili, J., Keko, H., Mendes, J., Bessa, R.J., Miranda, V.: Demand dispatch and probabilistic wind power forecasting in unit commitment and economic dispatch: a case study of illinois. IEEE Trans. Sustain. Energy **4**(1), 250–261 (2013)
5. Matos, M.A., Bessa, R.J.: Setting the operating reserve using probabilistic wind power forecasts. IEEE Trans. Power Syst. **26**(2), 594–603 (2011)
6. Kou, P., Gao, F., Guan, X.: Stochastic predictive control of battery energy storage for wind farm dispatching: using probabilistic wind power forecasts. Renew. Energy **80**, 286–300 (2015)
7. Botterud, A., Zhou, Z., Wang, J., Valenzuela, J., Sumaili, J., Bessa, R.J., Keko, H., Miranda, V.: Unit commitment and operating reserves with probabilistic wind power forecasts. In: 2011 IEEE Trondheim PowerTech, pp. 1–7, June 2011
8. Zhang, Y., Wang, J., Wang, X.: Review on probabilistic forecasting of wind power generation. Renew. Sustain. Energy Rev. **32**, 255–270 (2014)
9. Li, P., Guan, X., Wu, J.: Aggregated wind power generation probabilistic forecasting based on particle filter. Energy Convers. Manag. **96**, 579–587 (2015)
10. Huang, C.M., Huang, Y.C., Huang, K.Y., Chen, S.J., Yang, S.P.: Deterministic and probabilistic wind power forecasting using a hybrid method. In: 2017 IEEE International Conference on Industrial Technology (ICIT), pp. 400–405, March 2017
11. Wan, C., Lin, J., Wang, J., Song, Y., Dong, Z.Y.: Direct quantile regression for nonparametric probabilistic forecasting of wind power generation. IEEE Trans. Power Syst. **32**(4), 2767–2778 (2017)
12. Yan, J., Li, K., Bai, E.W., Deng, J., Foley, A.M.: Hybrid probabilistic wind power forecasting using temporally local gaussian process. IEEE Trans. Sustain. Energy **7**(1), 87–95 (2016)
13. Kou, P., Liang, D., Gao, F., Gao, L.: Probabilistic wind power forecasting with online model selection and warped Gaussian process. Energy Convers. Manag. **84**, 649–663 (2014)

14. Mangalova, E., Shesterneva, O.: K-nearest neighbors for GEFCom2014 probabilistic wind power forecasting. Int. J. Forecasting **32**(3), 1067–1073 (2016)
15. Zhang, Y., Wang, J.: K-nearest neighbors and a kernel density estimator for GEFCom2014 probabilistic wind power forecasting. Int. J. Forecasting **32**(3), 1074–1080 (2016)
16. Gallego-Castillo, C., Bessa, R., Cavalcante, L., Lopez-Garcia, O.: On-line quantile regression in the RKHS (reproducing kernel hilbert space) for operational probabilistic forecasting of wind power. Energy **113**, 355–365 (2016)
17. Aguilar, S., Souza, R.C., Pensanha, J.F.: Predicting probabilistic wind power generation using nonparametric techniques. In: 2014 International Conference on Renewable Energy Research and Application (ICRERA), pp. 709–712, October 2014
18. Wei, Z., Liu, S.M., Wei, D., Wang, Z.J., Yang, M.L., Li, Y.: Probabilistic wind power forecast using sparse Bayesian learning of unified kernel function. In: 2014 IEEE Conference and Expo Transportation Electrification Asia-Pacific (ITEC Asia-Pacific), pp. 1–4, August 2014
19. Lee, D., Baldick, R.: Probabilistic wind power forecasting based on the Laplace distribution and golden search. In: 2016 IEEE/PES Transmission and Distribution Conference and Exposition (TD), pp. 1–5, May 2016
20. Sideratos, G., Hatziargyriou, N.D.: Probabilistic wind power forecasting using radial basis function neural networks. IEEE Trans. Power Syst. **27**(4), 1788–1796 (2012)
21. Zhang, Y., Wang, J., Luo, X.: Probabilistic wind power forecasting based on logarithmic transformation and boundary kernel. Energy Convers. Manag. **96**, 440–451 (2015)
22. Carpinone, A., Langella, R., Testa, A., Giorgio, M.: Very short-term probabilistic wind power forecasting based on Markov chain models. In: 2010 IEEE 11th International Conference on Probabilistic Methods Applied to Power Systems, pp. 107–112, June 2010
23. Dowell, J., Pinson, P.: Very-short-term probabilistic wind power forecasts by sparse vector autoregression. IEEE Trans. Smart Grid **7**(2), 763–770 (2016)
24. Nasraoui, K., Lakhoua, N., Amraoui, L.E.: Study and analysis of micro smart grid using the modeling language SysML. In: 2017 International Conference on Green Energy Conversion Systems (GECS), pp. 1–8, March 2017
25. Lakhoua, M.: Systemic analysis of a wind power station in Tunisia. J. Electr. Electron. Eng. **4**, 83–88 (2011)
26. Do, C.B.: Gaussian Processes. Stanford University, Stanford (2007)
27. Meinshausen, N.: Quantile regression forests. J. Mach. Learn. Res. **7**, 983–999 (2006)
28. Weron, R.: Electricity price forecasting: a review of the state-of-the-art with a look into the future. Int. J. Forecasting **30**(4), 1030–1081 (2014)